SCIENTIFIC REPORTS
nature research

OPEN

Evolution of two bulk-superconducting phases in $Sr_{0.5}RE_{0.5}FBiS_2$ (*RE*: La, Ce, Pr, Nd, Sm) by external hydrostatic pressure effect

Aichi Yamashita[1], Rajveer Jha[1], Yosuke Goto[1], Akira Miura[2], Chikako Moriyoshi[3], Yoshihiro Kuroiwa[3], Chizuru Kawashima[4], Kouhei Ishida[4], Hiroki Takahashi[4] & Yoshikazu Mizuguchi[1]✉

Polycrystalline samples of $Sr_{0.5}RE_{0.5}FBiS_2$ (*RE*: La, Ce, Pr, Nd, and Sm) were synthesized via the solid-state reaction and characterized using synchrotron X-ray diffraction. Although all the $Sr_{0.5}RE_{0.5}FBiS_2$ samples exhibited superconductivity at transition temperatures (T_c) within the range of 2.1–2.7 K under ambient pressure, the estimated superconducting volume fraction was small, which indicates non-bulk nature of superconductivity in those samples under ambient pressure. A dramatic increase in shielding fraction, which indicates the emergence of the bulk superconductivity was achieved by applying external hydrostatic pressures. We found that two phases, low-*P* phases with T_c = 2.5–2.8 K and high-*P* phases with T_c = 10.0–10.8 K, were induced by the pressure effect for samples with RE = La, Ce, Pr, and Nd. Pressure-T_c phase diagrams indicated that the critical pressure for the emergence of the high-*P* phase tends to increase with decreasing ionic radius of the doped *RE* ions, which was explained by the correlation between external and chemical pressure effects. According to the high-pressure X-ray diffraction measurements of $Sr_{0.5}La_{0.5}FBiS_2$, a structural phase transition from tetragonal to monoclinic also occurred at approximately 1.1 GPa. Bulk superconducting phases in $Sr_{0.5}RE_{0.5}FBiS_2$ induced by the external hydrostatic pressure effect are expected to be useful for understanding the effects of both external and chemical pressures to the emergence of bulk superconductivity and pairing mechanisms in BiCh_2-based superconductors.

The discovery of superconductivity in BiS_2-based compounds[1,2] such as $Bi_4O_4S_3$ and $REO_{1-x}F_xBiS_2$ has triggered numerous studies focusing on identifying new superconductors featuring a higher transition temperatures (T_c) and elucidating the mechanisms of superconductivity in BiS_2-based compounds. Due to the similarity of the crystal structure among the BiS_2-based, cuprates and iron-based compounds[3,4], BiS_2-based compounds have been considered as a new example of layered superconductor family. Thus far, various types of BiS_2-based compounds have been synthesized by replacing different blocking layers[1,2,5–17], such as the $Bi_4O_4(SO_4)_{1-x}$ layer, the *REO* layer (*RE*: La, Ce, Pr, Nd, and Sm), or the *AE*F layer (*AE*: Sr or Eu). Notably, some BiS_2-based compounds do not exhibit bulk superconductivity even after electron doping. To induce bulk superconductivity in BiS_2-based compounds, various chemical substitutions have been attempted (see review articles)[14,18]. Among these, the isovalent substitutions, such as Nd^{3+} substitutions for La^{3+} or Se^{2-} substitutions for S^{2-}, were found to be effective for inducing bulk superconductivity. Based on systematic structural analyses, we have revealed that the in-plane chemical pressure is one of the essential parameters that facilitate the emergence of bulk superconductivity in

[1]Department of Physics, Tokyo Metropolitan University, 1-1 Minami-Osawa, Hachioji, Tokyo 192-0397, Japan. [2]Faculty of Engineering, Hokkaido University, Kita-13, Nishi-8, Kita-ku, Sapporo, Hokkaido 060-8628, Japan. [3]Graduate School of Advanced Science and Engineering, Hiroshima University, 1-3-1 Kagamiyama, Higashihiroshima, Hiroshima 739-8526, Japan. [4]Department of Physics, College of Humanities and Sciences, Nihon University, Setagaya, Tokyo 156-8550, Japan. ✉email: mizugu@tmu.ac.jp

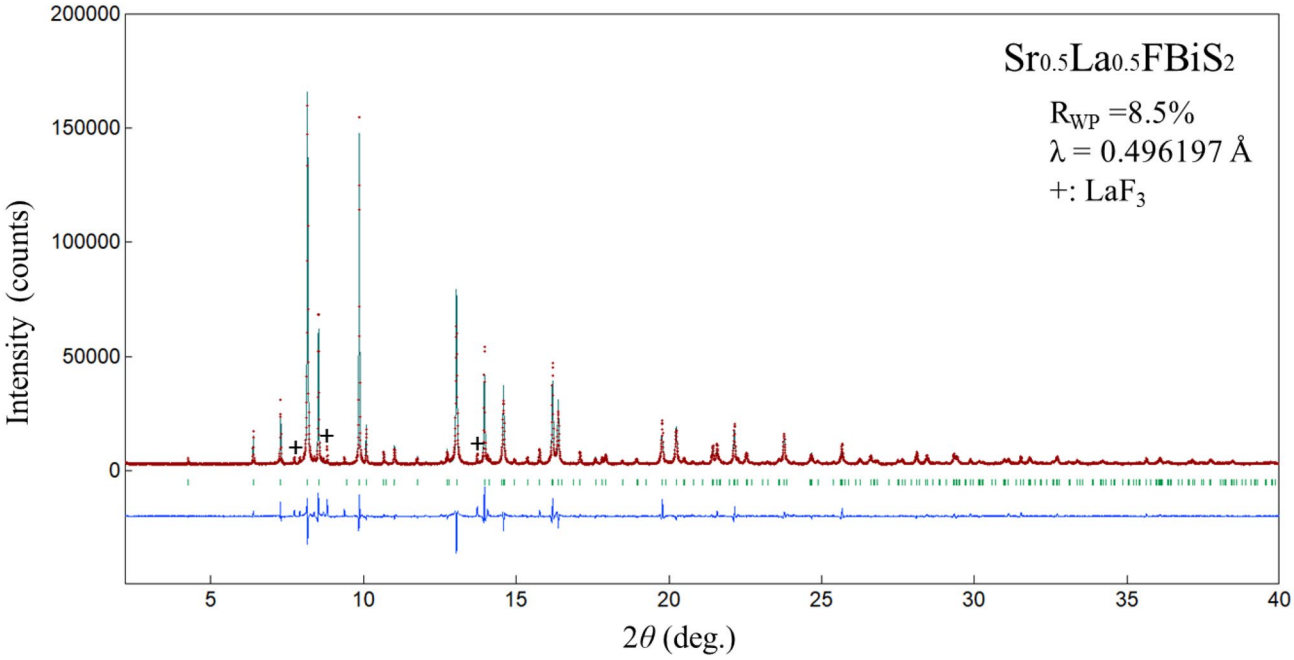

Figure 1. Synchrotron powder XRD patterns for $Sr_{0.5}La_{0.5}FBiS_2$. Symbol of + indicates the impurity of LaF_3.

BiCh_2-based (*Ch*: S, Se) systems[18,19]. By applying in-plane chemical pressure, the local structural disorder in the tetragonal structure is removed, and bulk superconductivity is induced[20,21]. To induce bulk superconductivity, external pressure effects are also effective[22–32]. For $REO_{0.5}F_{0.5}BiS_2$ and $EuFBiS_2$, the T_c at ambient condition (~ 2.5 K and ~ 0.5 K) dramatically increase to ~ 10 K under high pressure[23–26], and the origin of the increase in T_c was explained by a structural transition from tetragonal ($P4/nmm$) to monoclinic ($P2_1/m$) at around 1 GPa for $LaO_{0.5}F_{0.5}BiS_2$ and $EuFBiS_2$[23,24]. In spite of the interesting phenomena under high pressure in those BiS_2-based compounds, the pressure studies have been performed by electrical resistivity measurements. To the best of our knowledge, only two works have used magnetization as a probe for the pressure studies, which confirmed bulk superconductivity in $LaO_{0.5}F_{0.5}BiS_2$ and $EuFBiS_2$ under high pressure[23,24]. Therefore, further experiments on how the bulk characteristics of superconductivity could be achieved under pressures are needed. In addition, as summarized above, there are two ways, chemical and external pressure effects, to induce bulk superconductivity. Note that those two bulk superconducting phases have a different crystal structure system of tetragonal (under chemical pressure) and monoclinic (under external pressure). Therefore, in order to further investigate the interplay among superconducting characteristics (T_c and bulk nature), external pressure, and chemical pressure, it is essential to establish a new system where discussion about the relationships among those factors is possible. In this study, to search for a system which enables us to study such relationships, we have studied the chemical and external pressure effects for the $Sr_{0.5}RE_{0.5}FBiS_2$ (*RE*: La, Ce, Pr, Nd, and Sm) system.

$SrFBiS_2$ is a parent phase of those target materials and a semiconductor with a band gap. The substitution of Sr^{2+} with RE^{3+} induces electron carriers in the BiS_2 layer, and filamentary superconductivity appears at approximately 2.8 K in La-, Ce-, and Pr-doped compounds[12–15,29–32]. Based on electrical resistivity measurements conducted under high pressures, a considerable increase in T_c was observed in previous pressure experiments[22,29–32]. The highest T_c in $Sr_{0.5}RE_{0.5}FBiS_2$ is approximately 10 K, and the pressure dependences of T_c exhibits a sharp increase at the critical pressure (~ 1 GPa). Since there has been no further report on the pressure-induced superconductivity in $Sr_{0.5}RE_{0.5}FBiS_2$, we have studied the superconducting phase diagrams for $Sr_{0.5}RE_{0.5}FBiS_2$ from magnetization experiments under high pressure and discussed the interplay among superconducting characteristics, chemical pressure, and external pressure. Two bulk superconducting phases with a lower T_c (low-P phase) and a higher T_c (high-P phase) were confirmed.

Results

Sample characterization and physical properties at ambient pressure. Figure 1 depicts the powder synchrotron X-ray diffraction (XRD) patterns for $Sr_{0.5}La_{0.5}FBiS_2$. For $Sr_{1-x}RE_xFBiS_2$ (*RE* = Ce, Pr, Nd, and Sm), see Supplemental Fig. S1a–d. The crystal structure of the obtained samples was well refined using the Rietveld method. They were well refined using a tetragonal structure with the $P4/nmm$ space group. Small impurity peaks due to REF_3 (*RE*: La, Ce) and Bi_2S_3 were also detected in the case of the Pr-, Nd-, and Sm-based samples. As shown in Fig. 2, we observed that the lattice constant a decreased with decreasing *RE* ionic radius; however, the lattice constant c increased under these conditions. The obtained values were in agreement with previous reports[12,30,31]. The chemical composition ratios of the samples were determined using energy dispersive X-ray spectroscopy (EDX). These results showed that the chemical compositions of the obtained samples were in reasonable agreement with the nominal compositions (Table 1). The electrical resistivity of the samples at ambient pressure was measured down to 1.6 K (Fig. 3). In all the samples, semiconducting behaviour was observed;

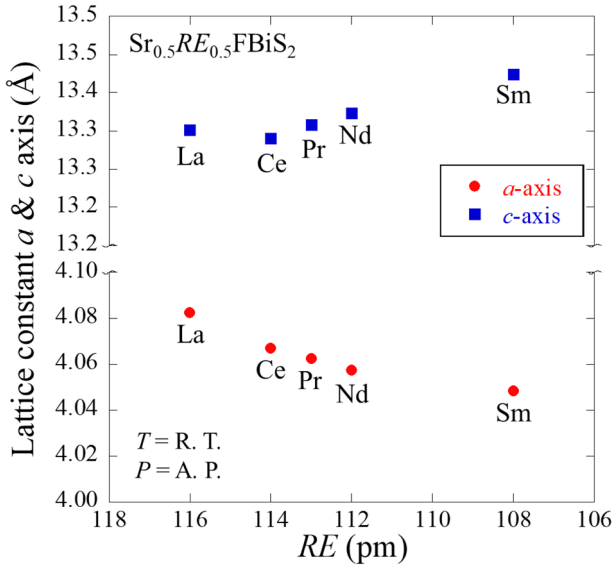

Figure 2. Dependences of the lattice constants *a* and *c* as a function of the RE^{3+} (*RE*: La, Ce, Pr, Nd, and Sm) ionic radius.

Nominal composition	Actual composition
$Sr_{0.50}La_{0.50}FBiS_2$	$Sr_{0.52}La_{0.48}FBi_{1.00}S_{2.00}$
$Sr_{0.50}Ce_{0.50}FBiS_2$	$Sr_{0.54}Ce_{0.48}FBi_{0.98}S_{2.00}$
$Sr_{0.50}Pr_{0.50}FBiS_2$	$Sr_{0.56}Pr_{0.41}FBi_{0.99}S_{2.04}$
$Sr_{0.50}Nd_{0.50}FBiS_2$	$Sr_{0.60}Nd_{0.39}FBi_{0.98}S_{2.03}$
$Sr_{0.50}Sm_{0.50}FBiS_2$	$Sr_{0.64}Sm_{0.39}FBi_{0.97}S_{2.01}$

Table 1. Actual composition (mol%) from the EDX analysis against the nominal composition (mol%). Fluorine amount is regarded as 1.

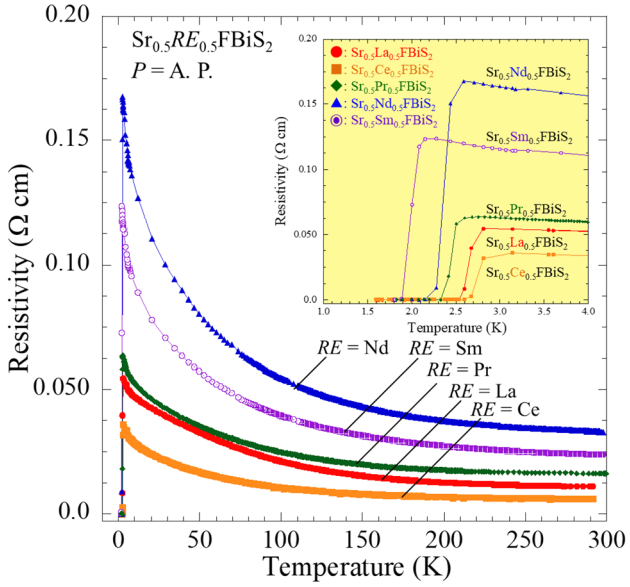

Figure 3. Temperature dependence of resistivity for $Sr_{0.5}RE_{0.5}FBiS_2$ (*RE*: La, Ce, Pr, Nd, and Sm) at ambient pressure. A. P. denotes an ambient pressure condition.

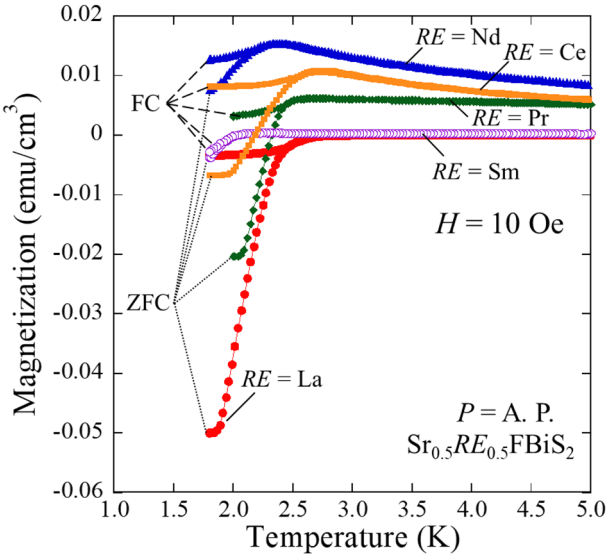

Figure 4. Temperature dependence of magnetization for $Sr_{0.5}RE_{0.5}FBiS_2$ (*RE*: La, Ce, Pr, Nd, and Sm) at ambient pressure. Dashed and dotted lines indicate a field cooling (FC) and zero-field cooling (ZFC), respectively. A. P. denotes an ambient pressure condition.

moreover, the resistivity-temperature (ρ-T) curve indicated a slight increase in ρ on cooling, which implied that the conduction electrons were weakly localized due to the in-plane local disorder in the BiS_2 layer[18–21]. A superconducting transition was observed at $T_c = 2.7$, 2.7, 2.6, 2.6, and 2.1 K for RE = La, Ce, Pr, Nd, and Sm, respectively (see the inset of Fig. 3). In addition, a superconducting transition was also observed in the temperature dependence of magnetization, as plotted in Fig. 4. The T_c estimated based on magnetization was in agreement with that obtained based on the resistivity measurements. This is the first study to report on the observation of superconductivity in $Sr_{0.5}Nd_{0.5}FBiS_2$ and $Sr_{0.5}Sm_{0.5}FBiS_2$ under ambient pressure. However, in these samples, the estimated shielding volume fraction was less than 6%. This indicates that chemical pressure effects, which is expected to be generated by the substitution of smaller *RE* such as Nd and Sm, are insufficient to induce bulk superconductivity in the $Sr_{1-x}RE_xFBiS_2$ system. To obtain bulk superconductivity, which is essentially important for describing intrinsic superconducting properties, we applied external pressure on the samples.

External pressure effect. Figure 5a shows the temperature dependences of the magnetization of $Sr_{0.5}La_{0.5}FBiS_2$ when increasing the applied pressure to 1.15 GPa. The T_c of approximately 2.7 K (low-P phase) remained almost unchanged up to 0.84 GPa; alternatively, there was an evident increase in the shielding volume fraction. This result indicates that the external pressure effectively enhances the shielding volume fraction, which corresponds to the emergence of bulk nature of the superconducting states in the $Sr_{0.5}La_{0.5}FBiS_2$ samples at a low-P regime. A remarkable increase in T_c up to $T_c^{max} = 10.8$ K (high-P phase) was observed at $P > 0.95$ GPa. The enhancement in the shielding volume fraction was also observed in the high-P phase, which was achieved by increasing applied pressure to the maximum pressure, without a noticeable change in the T_c. The drastic increase in T_c is explained by a tetragonal to a monoclinic phase.

Figure 6a presents the laboratory X-ray diffraction patterns of $Sr_{0.5}La_{0.5}FBiS_2$ at room temperature under various applied pressures of up to 3.4 GPa. Shifts of the (001) and (004) peaks to higher angles clearly indicate the shrinkage of the lattice along the c-axis due to the pressure. In contrast, a relatively smaller shift of the (110) peak was detected, which indicates that the in-plane size remains almost unchanged. Strong peak broadening was observed for the (200) peak above 1.1 GPa, indicating peak splitting due to the lowering of in-plane structural symmetry. Similar peak splitting on the (200) peak was observed for isostructural $LaO_{0.5}F_{0.5}BiS_2$ and $EuFBiS_2$ samples under high pressure[23,24], and a resultant structural transition from a tetragonal to monoclinic phase was detected. We noticed that the (200) peak asymmetrically split into two or more peaks, as depicted in Fig. 6b. This unexpected evolutions of the XRD pattern may be due to the inhomogeneity of applied pressure and the flexible nature of the in-plane structure of BiS_2-based compounds. The critical pressure of 1.1 GPa estimated from the XRD corresponds satisfactorily with the P_c estimated from the magnetization measurements. To further analyse crystal structure of this phase under pressure, synchrotron XRD experiments under homogeneous pressure conditions are needed.

The pressure dependence of T_c is summarized in Fig. 5f; the light blue, blue, and pink regions indicate the filamentary superconductivity, bulk superconductivity in the low-P phase, and bulk superconductivity in the high-P phase, respectively. The low-P phase shifts to the high-P phase when a pressure slightly exceeding the critical pressure (P_c) for the high-P phase is applied. In regard to this, a phase diagram was created using the shielding volume fraction of 20% or more as a bulk state in order to discuss the phase transition. In the pressure range of 0–0.84 GPa, $T_c(P)$ remains almost constant (~ 2.7 K). The bulk superconductivity of the sample was induced by

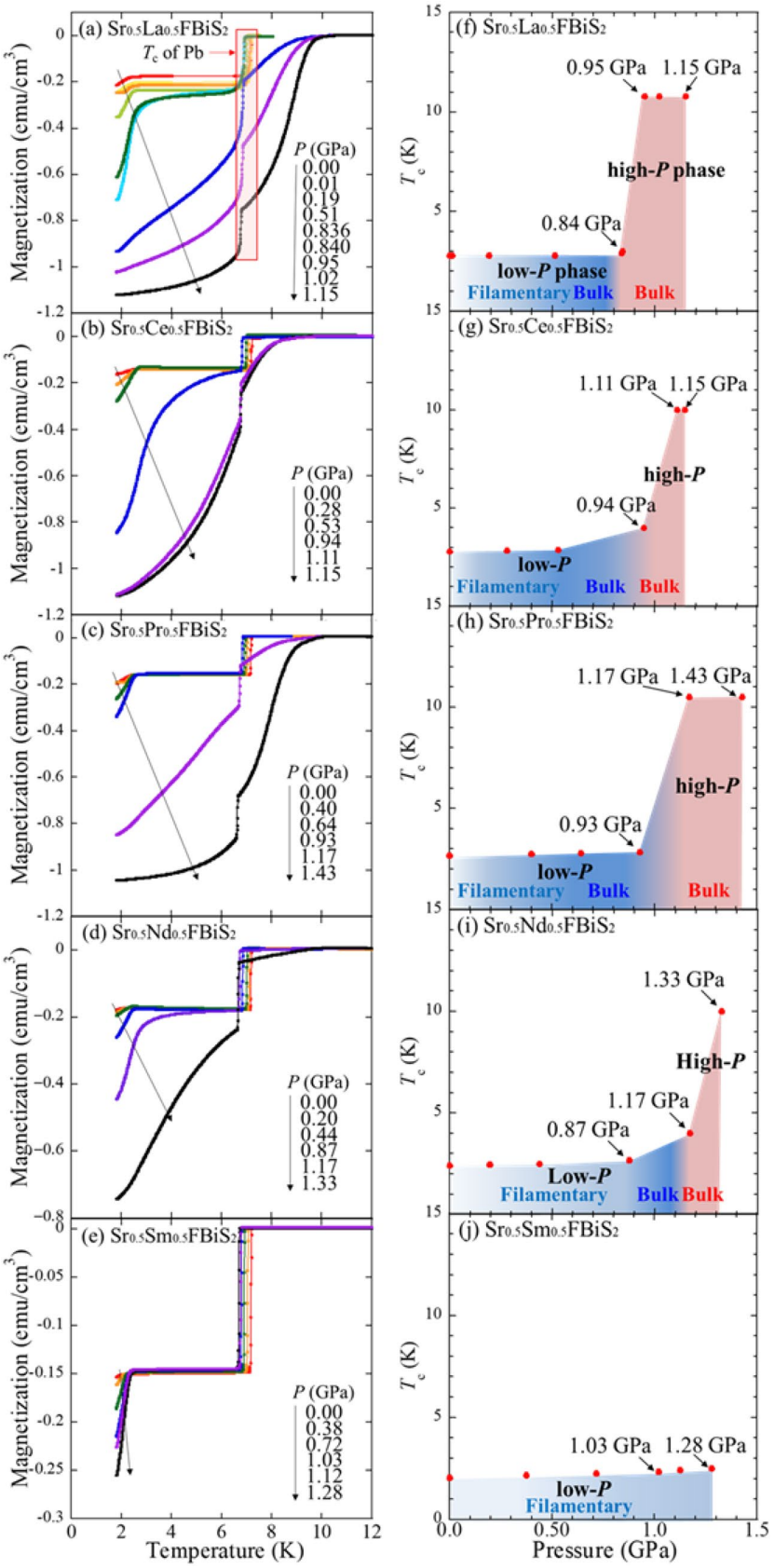

Figure 5. (**a**–**e**) Temperature dependences of magnetization under various pressure (P_{La} = 0, 0.01, 0.19, 0.51, 0.836, 0.840, 0.95, 1.02, and 1.15 GPa; P_{Ce} = 0, 0.28, 0. 53 0.94, 1.11, and 1.15 GPa; P_{Pr} = 0.0, 0.40, 0.64, 0.93, 1.17, and 1.43 GPa; P_{Ndr} = 0.0, 0.20, 0.44, 0.87, 1.17, and 1.33 GPa; P_{Sm} = 0.0, 0.375, 0.716, 1.03, 1.12, and 1.28 GPa) for $Sr_{0.5}RE_{0.5}FBiS_2$ (*RE*: La, Ce, Pr, Nd, and Sm), (**f**–**j**) pressure dependence of T_c for $Sr_{0.5}RE_{0.5}FBiS_2$ (*RE*: La, Ce, Pr, Nd, and Sm) when a magnetic field of 10 Oe was applied for all samples. The superconducting transition around 7 K indicates the superconducting transition of Pb manometer.

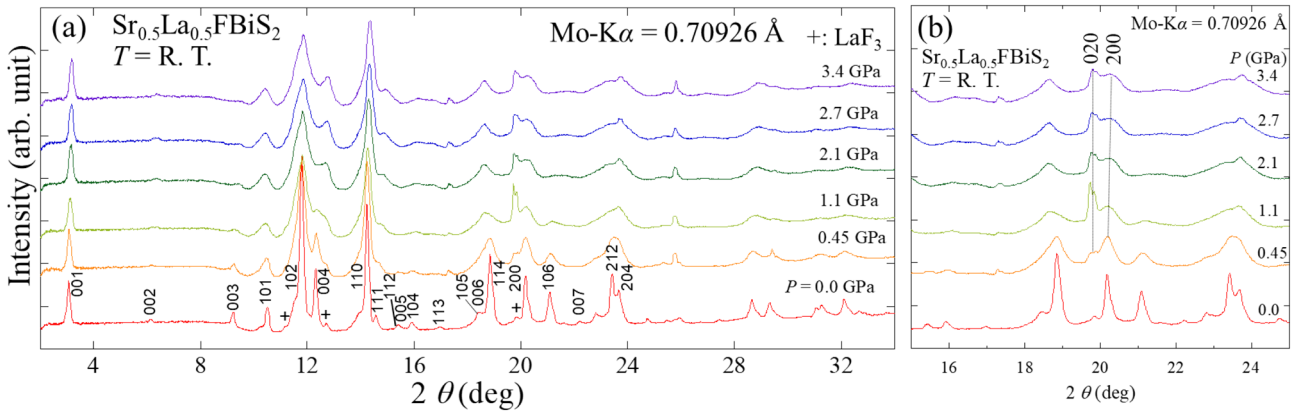

Figure 6. (**a**) XRD patterns (Mo K_α) of $Sr_{0.5}La_{0.5}FBiS_2$ under various pressure at room temperature. (**b**) Zoomed XRD patterns near the 020 and 200 peaks.

the pressure for the low-P phase region; eventually, the high-P phase region emerged at approximately $P = 0.95$ GPa with the bulk superconducting states. The $T_c(P)$ for the high-P phase region is almost constant (10.8 K).

The temperature dependence of magnetization under pressure and the pressure dependence of T_c phases for all the samples with different RE are summarized in Fig. 5a–j and respectively. The high-P phase of $Sr_{0.5}Sm_{0.5}FBiS_2$ was not observed up to 1.28 GPa, which is nearly the upper limit of the pressure measurement apparatus used in this experiment. This is the first report offering evidence of the bulk nature of two different (low-P and high-P) phases of the $Sr_{1-x}RE_xFBiS_2$ (RE: La, Ce, Pr, and Nd) superconductors when subjected to pressure.

Discussion

In this section, we discuss the relationship between external pressure effects, chemical pressure effects, and evolution of superconductivity in $Sr_{0.5}RE_{0.5}FBiS_2$. On comparing the evolutions of superconductivity for RE = Ce–Sm and that for RE = La, a slight decrease in T_c for the low-P phase was observed with increasing pressure for the RE = Ce, Pr, Nd and, Sm samples. Similar trend was observed in a phase diagram of tetragonal phase of BiCh_2-based systems examined as a function of chemical pressure[18,19,33]. Moreover, we observed that the T_c of the high-P phase showed a trend of decreasing with decreasing RE ionic radius. This trend is also common to that observed in high-pressure studies for $REO_{0.5}F_{0.5}BiS_2$ with different RE[22]. The P_c increased with decreasing RE ionic radius. Specifically, P_c was roughly estimated as 0.95, 1.11, 1.17, and 1.33 GPa for La^{3+} (with an ionic radius of 1.16 Å), Ce^{3+} (with an ionic radius of 1.14 Å), Pr^{3+} (with an ionic radius of 1.13 Å), and Nd^{3+} (with an ionic radius of 1.11 Å), respectively, where those ionic radii are values for a coordination number of 8. We noticed that the shift in P_c by replacing RE in $Sr_{0.5}RE_{0.5}FBiS_2$ is clearly small as compared to the case of $REO_{0.5}F_{0.5}BiS_2$; P_c was ~ 2 GPa for $NdO_{0.5}F_{0.5}BiS_2$[28]. These trends, the increase in P_c and the decrease in T_c with a decrease in RE ionic radius, were also observed for $REO_{0.5}F_{0.5}BiS_2$ compounds[22,26,28]; specifically, the T_c varied from approximately 10 to 6 K. The different pressure evolutions of superconducting phases in between the $Sr_{0.5}RE_{0.5}FBiS_2$ and $REO_{0.5}F_{0.5}BiS_2$ systems would be understood by the difference in the substitution sites. For $Sr_{0.5}RE_{0.5}FBiS_2$, the Sr site is partly (50%) substituted by RE, and hence the Sr-F bonds are partly remained. In the case of $REO_{0.5}F_{0.5}BiS_2$, all the RE site is replaced by different RE, and hence the RE-(O,F) bond length should systematically decrease according to the RE ionic radius. Therefore, the different sensitivity of the crystal structure and superconductivity to external pressures were observed between $Sr_{0.5}RE_{0.5}FBiS_2$ and $REO_{0.5}F_{0.5}BiS_2$. The difference should be caused by the chemical bonding states of the SrF-based and REO-based layers and the interlayer interaction between the blocking layers and BiS_2 conducting layers. Our results suggest that the structure of the blocking layer largely affects the evolution of superconducting phases under high pressures. The results obtained in this study will be useful for material design of BiCh_2-based superconductors with a higher T_c.

Conclusion

We showed the results of the synthesis, crystal structure analysis, resistivity, and magnetic susceptibility measurements investigated under ambient and high pressures for $Sr_{0.5}RE_{0.5}FBiS_2$ (RE: La, Ce, Pr, Nd, and Sm). The effects of external pressure on magnetization resulted in abrupt increments in T_c up to 10–10.8 K for the samples with RE = La, Ce, Pr, and Nd. Based on the analyses of the shielding volume fraction estimated via magnetic susceptibility measurements, we found that two bulk superconducting phases (low-P and high-P phases) can be induced by external pressure for $Sr_{0.5}RE_{0.5}FBiS_2$. For RE = La, we have confirmed a structural transition from laboratory XRD under high pressure, which is a common trend with those observed for $LaO_{0.5}F_{0.5}BiS_2$ and $EuFBiS_2$. The critical pressure, where T_c sharply increased to the high-P phase, shifted to a higher pressure with decreasing RE ionic radius. This implied that both the external and chemical pressures were affecting T_c. In addition, we have compared the obtained phase diagrams for $Sr_{0.5}RE_{0.5}FBiS_2$ and $REO_{0.5}F_{0.5}BiS_2$. We found differences in the sensitivity of the crystal structure and superconducting characteristics to external pressure effects between $Sr_{0.5}RE_{0.5}FBiS_2$ and $REO_{0.5}F_{0.5}BiS_2$, which should be caused by the different chemical bonding states in the blocking layers and the interlayer interaction between the blocking layers and BiS_2 conducting layers.

Methods

Polycrystalline $Sr_{0.5}RE_{0.5}FBiS$ (*RE*: La, Ce, Pr, Nd, and Sm) samples were synthesized by solid state reaction method in an evacuated quartz tube. Powders of RE_2S_3 (*RE*: La (99.9%), Ce (99.9%), Pr (99%), Nd (99%), and Sm (99.9%)), SrF_2 (99%), Bi (99.999%), and S (99.9999%) were weighed for $Sr_{0.5}RE_{0.5}FBiS_2$. The mixed powder was subsequently pelletized, sintered in an evacuated quartz tube at 700 °C for 20 h, followed by furnace cooling to room temperature. The obtained compounds were thoroughly mixed and ground, then sintered in the same conditions as the first sintering.

The phase purity and the crystal structure of the $Sr_{0.5}RE_{0.5}FBiS_2$ (*RE*: La, Ce, Pr, Nd, and Sm) samples were examined by powder synchrotron XRD (ambient pressure XRD) with an energy of 25 keV ($\lambda = 0.49657$ Å) at the beamline BL02B2 of SPring-8 under a proposal No. 2019A1101. The synchrotron XRD experiments were performed at room temperature with a sample rotator system, and the diffraction data were collected using a high-resolution one-dimensional semiconductor detector MYTHEN [Multiple mythen system] with a step of $2\theta = 0.006°$. To investigate the evolution of crystal structure of $Sr_{0.5}La_{0.5}FBiS_2$, laboratory XRD experiments under high pressure up to 3.4 GPa were performed at room temperature using a Mo-K_α radiation on a Rigaku (MicroMax-007HF) rotating anode generator equipped with a 100 μm collimator. Daphne 7474 was used as a pressure medium.

The crystal structure parameters were refined using the Rietveld method with a RIETAN-FP software[34]. The actual compositions of the obtained samples were analysed using an energy dispersive X-ray spectroscopy (EDX) on TM-3030 (Hitachi).

The temperature dependence of magnetic susceptibility at ambient pressure and under high pressures were measured using a superconducting quantum interference devise (SQUID) with MPMS-3 (Quantum Design). Hydrostatic pressures were generated by the MPMS high pressure Capsule Cell. The sample was immersed in a pressure transmitting medium (Daphene 7373) covered with a Teflon cell. The pressure at low temperature was calibrated from the superconducting transition temperature of Pb manometer. The electrical resistivity was measured on a GM refrigerator system (Made by Axis) using a conventional four-probe method. For the resistivity measurements, gold wires were connected to the samples with a silver paste.

Received: 15 June 2020; Accepted: 21 July 2020
Published online: 30 July 2020

References

1. Mizuguchi, Y. *et al.* BiS_2-based layered superconductor $Bi_4O_4S_3$. *Phys. Rev. B* **86**, 220510(R) (2012).
2. Mizuguchi, Y. *et al.* Superconductivity in novel BiS_2-based layered superconductor $LaO_{1-x}F_xBiS_2$. *J. Phys. Soc. Jpn.* **81**, 114725 (2012).
3. Bednorz, J. G. & Müller, K. A. Possible high T_c superconductivity in the Ba-La-Cu-O system. *Z. Phys. B* **64**, 189–193 (1986).
4. Kamihara, Y. *et al.* Iron-based layered superconductor $La[O_{1-x}F_x]FeAs$ (x = 0.05–0.12) with Tc = 26 K. *J. Am. Chem. Soc.* **130**, 3296–3297 (2008).
5. Singh, S. K. *et al.* Bulk superconductivity in bismuth oxysulfide $Bi_4O_4S_3$. *J. Am. Chem. Soc.* **134**, 16504–16507 (2012).
6. Demura, S. *et al.* BiS_2-based superconductivity in F-substituted $NdOBiS_2$. *J. Phys. Soc. Jpn.* **82**, 1–3 (2013).
7. Jha, R. *et al.* Synthesis and superconductivity of new BiS_2 based superconductor $PrO_{0.5}F_{0.5}BiS_2$. *J. Supercond. Nov. Magn.* **26**, 499–502 (2013).
8. Jha, R. *et al.* Superconductivity at 5 K in $NdO_{0.5}F_{0.5}BiS_2$. *J. Appl. Phys.* **113**, 056102 (2013).
9. Xing, J. *et al.* Superconductivity appears in the vicinity of an insulating-like behavior in $CeO_{1-x}F_xBiS_2$. *Phys. Rev. B* **86**, 214518 (2012).
10. Yazici, D. *et al.* Superconductivity of F-substituted $LnOBiS_2$ (*Ln* = La, Ce, Pr, Nd, Yb) compounds. *Philos. Mag.* **93**, 673 (2012).
11. Yazici, D. *et al.* Superconductivity induced by electron doping in $La_{1-x}M_xOBiS_2$ (*M* = Ti, Zr, Hf, Th). *Phys. Rev. B* **87**, 174512 (2013).
12. Lin, X. *et al.* Superconductivity induced by La doping in $Sr_{1-x}La_xFBiS_2$. *Phys. Rev. B* **87**, 020504 (2013).
13. Mizuguchi, Y. Review of superconductivity in BiS_2-based layered materials. *J. Phys. Chem. Solids* **84**, 34–48 (2015).
14. Li, L. *et al.* Coexistence of superconductivity and ferromagnetism in $Sr_{0.5}Ce_{0.5}FBiS_2$. *Phys. Rev. B* **91**, 014508 (2015).
15. Sakai, H. *et al.* Insulator-to-superconductor transition upon electron doping in a BiS_2-based superconductor $Sr_{1-x}La_xFBiS_2$. *J. Phys. Soc. Jpn.* **83**, 014709 (2014).
16. Lei, H. *et al.* New layered fluorosulfide $SrFBiS_2$. *Inorg. Chem.* **52**, 10685–10689 (2013).
17. Goto, Y., Sogabe, R. & Mizuguchi, Y. Bulk superconductivity induced by Se substitution in $BiCh_2$-based layered compounds $Eu_{0.5}Ce_{0.5}FBiS_{2-x}Se_x$. *J. Phys. Soc. Jpn.* **86**, 104712 (2017).
18. Mizuguchi, Y. Material development and physical properties of BiS_2-based layered compounds. *J. Phys. Soc. Jpn.* **88**, 041001 (2019).
19. Mizuguchi, Y. *et al.* In-plane chemical pressure essential for superconductivity in $BiCh_2$-based (*Ch*: S, Se) layered structure. *Sci. Rep.* **5**, 14968 (2015).
20. Mizuguchi, Y. *et al.* Evolution of anisotropic displacement parameters and superconductivity with chemical pressure in BiS_2-Based $REO_{0.5}F_{0.5}BiS_2$ (RE = La, Ce, Pr, and Nd). *J. Phys. Soc. Jpn.* **87**, 023704 (2018).
21. Paris, E. *et al.* Role of the local structure in superconductivity of $LaO_{0.5}F_{0.5}BiS_{2-x}Se_x$ system. *J. Phys. Condens. Matter* **29**, 145603 (2017).
22. Jha, R. & Awana, V. P. S. Effect of hydrostatic pressure on BiS_2-based layered superconductors: A review. *Nov. Supercond. Mater.* **2**, 16–31 (2016).
23. Tomita, T. *et al.* Pressure-induced enhancement of superconductivity and structural transition in BiS_2-layered $LaO_{1-x}F_xBiS_2$. *J. Phys. Soc. Jpn.* **83**, 063704 (2014).
24. Guo, C. Y. *et al.* Evidence for two distinct superconducting phases in $EuBiS_2F$ under pressure. *Phys. Rev. B* **91**, 214512 (2015).
25. Kotegawa, H. *et al.* Pressure study of BiS_2-based superconductors $Bi_4O_4S_3$ and La(O, F)BiS_2. *J. Phys. Soc. Jpn.* **81**, 103702 (2012).
26. Wolowiec, C. T. *et al.* Pressure-induced enhancement of superconductivity and suppression of semiconducting behavior in $LnO_{0.5}F_{0.5}BiS_2$ (Ln = La, Ce) compounds. *Phys. Rev. B* **88**, 064503 (2013).
27. Jha, R., Kishan, H. & Awana, V. P. S. Effect of hydrostatic pressures on the superconductivity of new BiS_2 based $REO_{0.5}F_{0.5}BiS_2$ (RE=La, Pr and Nd) superconductors. *J. Phys. Chem. Solid* **84**, 17–23 (2015).
28. Wolowiec, C. T. *et al.* Enhancement of superconductivity near the pressure-induced semiconductor–metal transition in the BiS_2-based superconductors $LnO_{0.5}F_{0.5}BiS_2$ (Ln = La, Ce, Pr, Nd). *J. Phys. Condens. Matter* **25**, 422201 (2013).
29. Jha, R., Tiwari, B. & Awana, V. P. S. Impact of hydrostatic pressure on superconductivity of $Sr_{0.5}La_{0.5}FBiS_2$. *J. Phys. Soc. Jpn.* **83**, 063707 (2014).

30. Jha, R., Tiwari, B. & Awana, V. P. S. Appearance of bulk superconductivity under hydrostatic pressure in $Sr_{0.5}RE_{0.5}FBiS_2$ (RE = Ce, Nd, Pr, and Sm) compounds. *J. Appl. Phys.* **117**, 013901 (2015).
31. You, W. *et al.* Superconductivity, electronic phase diagram, and pressure effect in $Sr_{1-x}Pr_xFBiS_2$. *Sci. China-Phys. Mech. Astron.* **62**, 957411 (2019).
32. Thakur, G. S. *et al.* Pressure enhanced superconductivity at 10 K in La doped $EuBiS_2F$. *Supercond. Sci. Technol.* **28**, 115010 (2015).
33. Jinno, G. *et al.* Bulk superconductivity induced by in-plane chemical pressure effect in $Eu_{0.5}La_{0.5}FBiS_{2-x}Se_x$. *J. Phys. Soc. Jpn.* **85**, 124708 (2016).
34. Izumi, F. & Momma, K. Three-dimensional visualization in powder diffraction. *Solid State Phenom.* **130**, 15–20 (2007).

Acknowledgements

The authors thank O. Miura for experimental supports. This work was partly supported by JSPS KAKENHI (Grant No. 18KK0076, 15H05886, and 19K15291) and Advanced Research Program under the Human Resources Funds of Tokyo (Grant Number: H31-1) and Nihon University President Grant Initiative.

Author contributions

A.Y. prepared all samples and did compositional analysis, resistivity, magnetization measurements. A.Y. measured magnetization under high pressure with the help of R. J. A. M., C. M. and Y. K. conducted powder synchrotron XRD measurements. C. K., K. I. and H. T. conducted the high-pressure XRD measurements. A.Y. and Y. M. wrote the manuscript and prepared all figures. Y. G. and Y. M. provided valuable suggestion for data analysis and corrected the manuscript. All authors contributed to discussion and reviewed the manuscript.

Competing interests

The authors declare no competing interests.

Additional information

Supplementary information is available for this paper at https://doi.org/10.1038/s41598-020-69889-w.

Correspondence and requests for materials should be addressed to Y.M.

Reprints and permissions information is available at www.nature.com/reprints.

Publisher's note Springer Nature remains neutral with regard to jurisdictional claims in published maps and institutional affiliations.